

See discussions, stats, and author profiles for this publication at: <https://www.researchgate.net/publication/8457998>

# Tapered Fiber Bundles for Combining High-power Diode Lasers

Article in *Applied Optics* · July 2004

DOI: 10.1364/AO.43.003893 · Source: PubMed

---

CITATIONS

35

---

READS

178

4 authors, including:



[Masud Mansuripur](#)

The University of Arizona

436 PUBLICATIONS 6,569 CITATIONS

SEE PROFILE

# Tapered fiber bundles for combining high-power diode lasers

Andrey Kosterin, Valery Temyanko, Mahmoud Fallahi, and Masud Mansuripur

Tapered fiber bundles are often used to combine the output power of several semiconductor lasers into a multimode optical fiber for the purpose of pumping fiber lasers and amplifiers. It is generally recognized that the brightness of such combiners does not exceed the brightness of the individual input fibers. We report that the brightness of the tapered fibers (and fiber bundles) depends on both the taper ratio and the mode-filling properties of the beams launched into the individual fibers. Brightness, therefore, can be increased by selection of sources that fill a small fraction of the input fiber's modal capacity. As proof of concept, we present the results of measurements on tapered fiber-bundle combiners having a low-output étendue. Under low mode-filling conditions per input multimode fiber (i.e., fraction of filled modes  $\leq 0.29$ ), we report brightness enhancements of 8.0 dB for  $19 \times 1$  bundles, 6.7 dB for  $7 \times 1$  bundles, and 4.0 dB for  $3 \times 1$  combiners. Our measured coupling efficiency variations of  $\sim 1\%$ – $2\%$  among the various fibers in a given bundle confirm the uniformity and quality of the fabricated devices. © 2004 Optical Society of America

OCIS codes: 060.2340, 060.1810, 140.2020, 140.2010.

## 1. Introduction

High-power laser diodes and laser-diode arrays are attractive light sources in applications ranging from laser machining to the pumping of other lasers. These applications require efficient beam-combining devices that equalize the optical invariants of the beam in orthogonal planes. In this regard, beam combiners that incorporate beam shaping have been discussed in the past.<sup>1–3</sup> These combiners are efficient but difficult to align and to maintain. Alternatively, multimode (MM) fiber-bundle and tapered fiber-bundle combiners, thanks to their inherent circular symmetry, are known to be homogeneous in both planes.<sup>4,5</sup> These bundles are ideal for the pumping of solid-state lasers and cladding-pumped fibers because of their reliability and ease of fabrication. It has also been demonstrated that these bundles can accommodate at their core a single-mode fiber for applications involving the pumping of single-mode (active) fibers.<sup>6,7</sup> A major drawback of fiber-coupled lasers (with or without bundling the fibers) is their

relatively low brightness.<sup>8</sup> For example, the radiance of a broad-stripe semiconductor laser (divergence angles  $10^\circ \times 40^\circ$ , corresponding to a  $1 \times 100 \mu\text{m}^2$  emitter area), when coupled to a MM step-index fiber having a  $100\text{-}\mu\text{m}$ -diameter core and a 0.22 numerical aperture (NA), is approximately 125 times lower than the radiance of the laser diode itself. Improving the coupling efficiency and brightness of MM fiber couplers or combiners is thus highly desirable.

It must be recognized in such applications that the MM fiber is generally operated under restricted-mode launch condition, that is, only a small fraction of the fiber's modal capacity is generally utilized. However, many coupler designs have traditionally required étendue invariance, namely,<sup>6,7</sup>

$$\left[ \sum_{i=1}^n A_i (NA_i)^2 \right]_{in} = A_{out} NA_{out}^2. \quad (1)$$

Here  $NA$  is the NA and  $A$  the cross-sectional area of input and output fibers. This is a necessary condition for maintaining low-loss transmission under the overfilled mode launch condition, where the modal content of the input source or sources is greater than or equal to the modal capacity of individual fibers. (Transmission properties of tapered MM optical fibers have been investigated, with ray-trace simulations, for a Lambertian source, which is a case of overfilled mode launch conditions.<sup>9</sup>) To the best of our knowledge, no data has been published on the

The authors are with the Optical Science Center, the University of Arizona, 1630 East University Boulevard, Tucson, Arizona 85718.

Received 27 August 2003; revised manuscript received 6 February 2004; accepted 30 March 2004.

0003-6935/04/193893-08\$15.00/0

© 2004 Optical Society of America

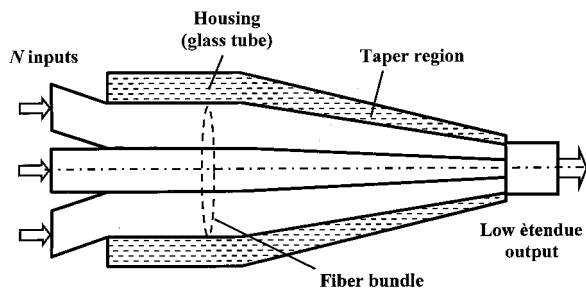


Fig. 1. Diagram of an  $N \times 1$  combiner, fabricated by fusing and tapering a fiber bundle. The beams of  $N$  laser diodes (either separate diodes or diodes from an array) enter from the left-hand side. The combined high-brightness beam emerges from the right.

throughput of tapered MM fibers and fiber bundles under restricted-mode launch conditions, where the modal content of the input source or sources is much smaller than the modal capacity of individual fibers.

In this paper we explore different beam-combining strategies based on tapered fiber bundles, aiming to increase the brightness of pump sources for double-clad fiber lasers and amplifiers. We consider single-stage  $N \times 1$  combiners with tapering and fusing of a conventional MM fiber bundle as well as multistage cascades of such  $N \times 1$  combiners. Our approach to brightness enhancement does not contradict the so-called radiance theorem,<sup>8</sup> because the laser-diode sources used in conjunction with our scheme operate in a restricted-mode condition, whereby they occupy only a fraction of the input fiber's modal capacity. We present throughput measurements of step-index MM fibers of differing taper ratios under (low-order) restricted-mode launch conditions. The results are compared with throughputs of the same (tapered) fibers under conditions that approach overfilled mode launch conditions, where high-order spatial modes are present (at significant levels) in the modal content of the input light source. (A comparison with theory for the overfilled mode launch conditions is given in Section 6.)

## 2. Experimental Conditions

Tapered fibers were fabricated with a modified pipette puller (Narishige Scientific Instruments PD-5 stage) that employs an oxygen–hydrogen torch as a heater, a gravitational force mechanism, a CCD camera, a microscope, and a side illuminator. Although the puller allows tapers with a maximum length of 32 mm, the most reproducible tapers were found to be in the range of 10–16 mm.

A standard Thorlabs MM fiber (AFS 105/125Y, 105- $\mu\text{m}$  fused-silica core, 125- $\mu\text{m}$  fluorine-doped cladding,  $NA = 0.22$ ) was the raw material in our experiments. With reference to Fig. 1, we put a fiber bundle consisting of 3, 4, 7, or 19 MM fibers through a quartz tube (Polymicro Technologies, LLC) and then fused the bundle together by inertially collapsing the tube softened by the torch. (The quartz tubes had different diameters to accommodate the desired number of fibers in each bundle.) In the first

stage of preparation only tight bundling was achieved. The taper was then pulled with simultaneous waist control while the taper was visually inspected through the microscope. The pulling stopped when the tapered end of the bundle matched the diameter of a standard MM fiber with reasonable tolerances. The fiber bundle was then cleaved at the tapered end.

Figure 2 shows cross-sectional photographs of typical tapered bundles thus obtained. The fused, tapered, and cleaved bundle was subsequently fusion spliced to a length of standard MM fiber; see Fig. 3. All tapers were adiabatic, and the taper ratio  $R = D'/D$ , which is the ratio of the fiber diameter  $D'$  at the end of the taper to the original fiber diameter,  $D = 125\ \mu\text{m}$ , ranged from slightly less than 0.2 to just less than 0.5. This range allows the fabrication of a number of fused and tapered fiber bundles [each bundle containing 3 ( $R = 0.49$ ), 4 ( $R = 0.42$ ), 7 ( $R = 0.317$ ) or 19 ( $R = 0.193$ ) fibers] that matched the  $\sim 105\text{-}\mu\text{m}$  core diameter of a standard MM fiber. (The aforementioned number of fibers in each bundle correspond to various close-packed configurations. Other configurations with different number of fibers per bundle are also possible but were not studied in this work.) Since our fabrication method yields a nearly constant taper angle of  $\Omega \sim 0.35^\circ$ , we achieved different  $R$  values by varying the length of the taper.

Three light sources were used in our experiments; these were fiber-coupled semiconductor laser diodes ( $\lambda = 980\ \text{nm}$ ) exhibiting different angular distributions of their emissions. Source 1 was a single-mode laser diode with a (single-mode) 0.11-NA fiber pigtail. The Gaussian-like far-field pattern of this source emerging from the pigtail fiber had a full-width divergence angle of  $\sim 12.6^\circ$ , as shown in Fig. 4. The pigtail was subsequently fusion spliced to a 1-m-long piece of standard MM fiber (AFS105/125Y). Source 2 utilized a SpectraPhysics BJ 234 laser diode (MM), collimated to better than  $1^\circ$  in its fast axis with a short length of optical fiber (glued to the laser body and acting as a cylindrical lens). The cleaved facet of a 1-m length of standard MM fiber was brought into proximity with the exterior face of the cylindrical lens (distance  $\sim 100\ \mu\text{m}$ ), thus permitting direct coupling of the laser beam into this MM fiber. The far-field distribution of source 2 that emerges from the 1-m-long fiber had full angular width (measured at the point where the amplitude drops to  $1/e$  of the peak amplitude) given by  $w \sim 13.9^\circ$ . Our restricted-mode launches were conducted with either source 1 or source 2.

The third light source, also based on a BJ 234 MM laser diode, was prism-coupled into a double-clad silica glass fiber (core/clad1/clad2 diameters = 6/90/125  $\mu\text{m}$ ) through a polished and flattened window on one side of the fiber; this fiber was then spliced into a 1-m-long MM fiber. The far-field pattern of source 3 had a full-width diameter  $w \sim 25^\circ$ , which filled the entire NA of the MM fiber. As will be seen below, the output of source 3 approaches that of a source that satisfies overfilled mode launch conditions.

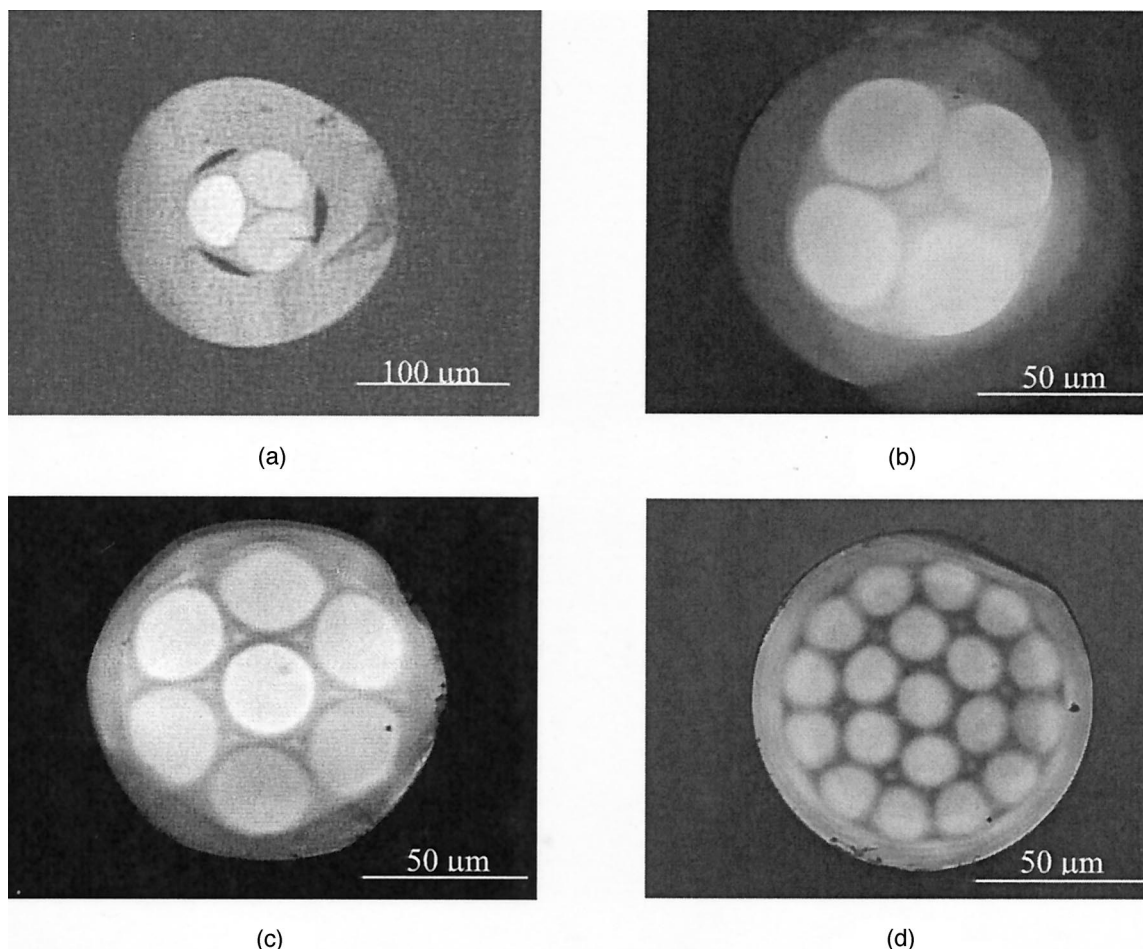


Fig. 2. Cross-sectional photographs of fused, tapered, and cleaved MM fiber bundles. (a)  $3 \times 1$  combiner; (b)  $4 \times 1$  combiner, (c)  $7 \times 1$  combiner, (d)  $19 \times 1$  combiner. Note that the empty spaces between adjacent fibers have been filled. The different gray levels of individual fibers within the bundle are caused by random illumination of their opposite ends.

Table 1 lists the characteristic parameters of our three sources, including the near-field diameter  $d$ , the full angular width  $w$ , and the estimated number of modes in the output beam  $V^2/2$ . The latter parameter is obtained from the expression

$$\frac{V^2}{2} = \pi^2 d^2 (w/2)^2 / 2\lambda^2. \quad (2)$$

After sources 1 and 2 have been propagated through the 1-m-long MM fibers, their modal content seems very similar to each other (as further verified by the coupling efficiency measurements described below). Source 3 is different from both sources 1 and 2 in that its modal space seems highly populated.

The far-field profiles of sources 2 and 3 were measured directly, using a Vidicon camera (Hamamatsu Model C2400) and neutral density filters, with the detector placed 17.5 mm away from the source. In the case of source 1, the presence of speckles after propagation through the 1-m-long MM fiber made it difficult to measure the near- and the far-field patterns. Table 1 thus lists for source 1 only the beam properties at the output of the single-mode pigtail

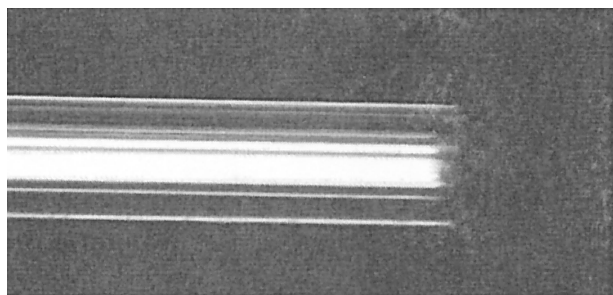
fiber. Mode filling, defined as the ratio of the number of filled modes over the fiber's modal capacity, was found to be  $\sim 0.29$  for sources 1 and 2 and  $\sim 1.0$  for source 3.

### 3. Beam Combiner Characteristics

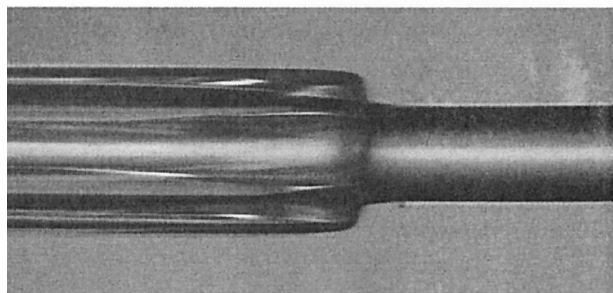
To study the feasibility of beam combining with fused and tapered MM fibers, we prepared several  $N \times 1$  combiners, shown in Fig. 2, and measured their transmission efficiency  $\eta_T$ . For maximum efficiency only adiabatic tapers were used. Our  $3 \times 1$  combiner, connected to either source 1 or source 2, showed an efficiency  $\eta_T \sim 83\%$  per input, thus confirming the feasibility of combining several high-power laser-diode beams into a bright spot of  $\sim 100\text{-}\mu\text{m}$  diameter. Interchannel differences of only 1%–2% indicate the high quality of these combiners. The transmission efficiency of our  $19 \times 1$  combiners, again measured with sources 1 and 2, was  $\eta_T \sim 30\%$  (per input). With 3.0-W laser diodes placed at its 19 input terminals, for example, we expect a total optical power of  $\sim 17.0$  W at the output facet (diameter  $\sim 100\text{-}\mu\text{m}$ ) of this combiner.

Figure 5 shows the measured transmission effi-





(a)



(b)

Fig. 3. (a) Side view of the tapered end of the fused, tapered, and cleaved  $4 \times 1$  MM fiber bundle of Fig. 2(b). (b) Cleaved facet of the tapered bundle in (a) is shown fusion-spliced to a MM fiber.

ciency (per input) as function of the taper ratio  $R$  for several fabricated combiners illuminated with source 2. In the case of the  $19 \times 1$  combiners (●) the taper ratio was about right, but the two  $7 \times 1$  combiners (▲), the  $4 \times 1$  combiner (■), and the  $3 \times 1$  combiner (◆) were overpulled, resulting in a smaller bundle (at the tapered end) than the core of the standard MM fiber. Despite this overpulling, the measured efficiencies, when plotted against the taper ratio  $R$ , are seen to exhibit the expected behavior indicated by the solid curve (see Section 5 for an explanation of the solid curve, which is the same as the upper curve of Fig. 9 below).

#### 4. Cascaded Tapered Fibers

We devised a simple method of analyzing the performance of  $N \times 1$  combiners and of cascades of such

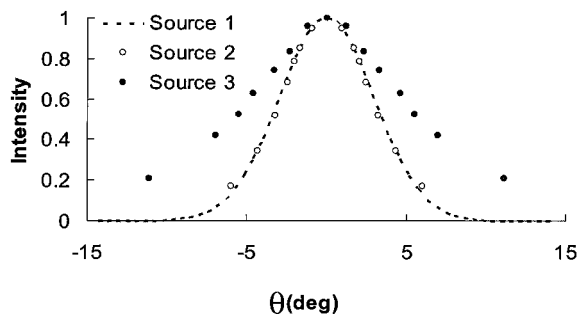


Fig. 4. Profiles of intensity distribution in the far field for the three sources used in our experiments. Source 1: dashed line, calculated; source 2: (○), measured; source 3: (●), measured.

Table 1. Source Characteristics and Estimated Number of Modes

Source	$V^2/2$	$d$ (μm)	$w$ (rad)
1 <sup>a</sup>	2	5.9	0.220
2	789	105	0.236
3	2742	105	0.440

<sup>a</sup>These characteristics of source 1 are based on the specifications of the pigtailed laser diode *before* the SM pigtail fiber is spliced to the 1-m-long MM fiber. After splicing, taper efficiencies measured with sources 1 and 2 seem the same for any value of the taper ratio  $R$ . This is an indication that sources 1 and 2, after being spliced to a 1-m-long MM fiber, launch approximately the same number of modes into the tapered fibers.

combiners. With reference to Fig. 6, we fabricated several nearly identical tapered fibers having the same taper ratio  $R$ , then measured the transmission efficiency  $\eta_T$  of a chain of such fibers in which each tapered fiber was fusion spliced to the next fiber at the center of its entrance facet (i.e., the unaltered facet). We emphasize that these were single tapered fibers, not bundles. All tapers were adiabatic, with the taper ratio  $R$  covering the range corresponding to combiners with 3, 4, 7, or 19 fibers in a bundle. To ensure that the results were not unduly influenced by propagation inside the cladding, we passed a loop of the output fiber through index-matching fluid (Cargille's Fused Silica Matching Liquid,) before measuring its output at the photodetector.

Figure 7 shows cascade efficiencies for chains of 1, 2, 3, and 4 fibers (all having the same taper ratio  $R = 0.26$ ,  $V = 19.3$ ), measured with source 1. Although there is loss at every stage, the first stage's loss is relatively small. The large efficiency,  $\eta_T = 47\%$ , obtained in the first stage of this cascade is due to the input beam having a limited modal content. After passing through the first tapered fiber, the beam divergence increases, causing the efficiency of transmission through the second stage to decrease to  $\sim 18\%$  (and the mode filling to increase). The rise in

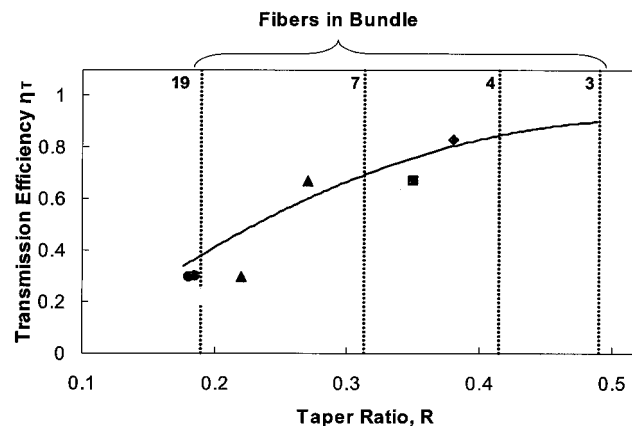


Fig. 5. Transmission efficiency  $\eta_T$  versus taper ratio  $R$  for several  $N \times 1$  combiners. (●)  $N = 19$ ; (▲)  $N = 7$ ; (■)  $N = 4$ ; (◆)  $N = 3$ . Some of the bundles were overpulled, resulting in a leftward shift of the corresponding data point on this plot. The solid curve is the best fit to the single taper's efficiency curve measured with source 2 (reproduced from Fig. 9).

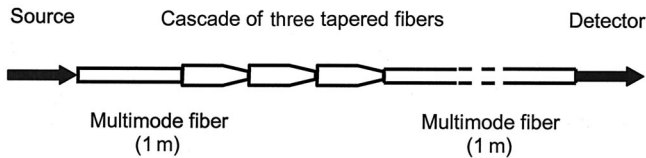


Fig. 6. Cascade of tapered fibers, all having the same taper ratio  $R$ , fusion spliced to each other and to 1-m-long pieces of the standard MM fiber on the input and the output sides. The light beam is launched into the 1-m-long input fiber. At the output side, a loop of the 1-m-long fiber is passed through index-matching fluid to remove any light that might be coupled into its cladding. The transmitted light is measured by the photodetector at the end of the output fiber. Although three tapered fibers are shown cascaded in this figure, the actual number in our experiments could be anywhere from one to four.

the modal content continues with passage through successive stages, resulting in  $\eta_T = 13\%$  for the third stage and  $\eta_T = 8\%$  for the fourth stage. For this last stage of the cascade, the input beam has approached a more or less overfilled mode condition, which leads to the correspondingly low transmission efficiency. The last taper efficiency is close to the  $R^2$  model prediction of 6.8% (see Section 6). The dashed horizontal line in Fig. 7 marks the 6.8% level. Any brightness enhancement, therefore, must occur in the earlier stages. The initial, restricted mode condition at the first stage (mode-filling parameter  $\sim 0.29$ ) has thus been transformed to an overfilled mode (mode-filling parameter  $\sim 1.0$ ) by the last stage.

For the above measurements to be relevant to our fused and tapered bundles, we must demonstrate that shifting the tapered (output) end of one fiber over the entrance facet of the succeeding fiber (as occurs for all but the central fiber in a cascaded bundle) does not seriously affect the throughput of the cascade pair. To this end, Fig. 8 shows the results of an experiment in which the tapered end of one fiber ( $R = 0.23$ ) was scanned across the entrance facet of an adjacent fiber. The two sets of measurements in Fig. 8 show the effect of core offset in the case of a tapered fiber displaced from the center of an output fiber (configuration A), and, in the case of a two-fiber

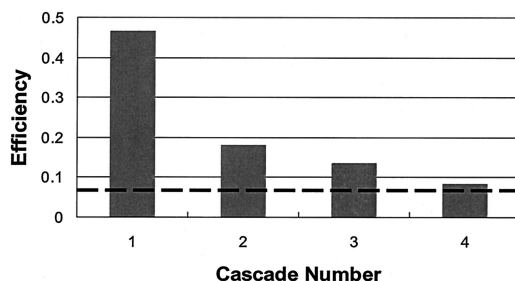


Fig. 7. Transmission efficiencies in a cascade of four tapered fibers. The taper ratio for all four fibers is  $R = 0.26$ . The light source is a single-mode laser coupled to a 1-m-long MM fiber (source 1). The transmission efficiency of the first stage is  $\eta_T \sim 47\%$ ; the remaining stages show progressively smaller efficiencies. The dashed line marks the 6.8% efficiency level corresponding to the overfilled mode condition.

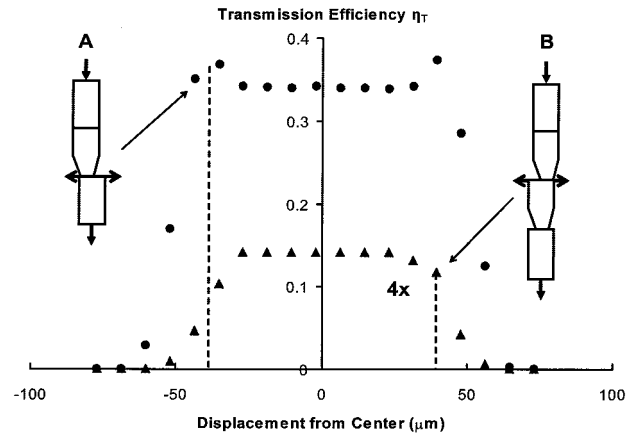


Fig. 8. Effect of core offset between the tapered end of one fiber and the untapered entrance facet of the next fiber in the cascade. In configuration A the transmission efficiency  $\eta_T$  is measured for a single taper, offset from the center of the 1-m-long output fiber, as a function of the displacement between the two cores. In configuration B, efficiency is measured for a cascade of two tapered fibers as a function of the core displacement of the first tapered fiber relative to the center of the second. In both cases the taper ratio was  $R = 0.23$ . The second curve is magnified by a factor of 4 to aid better visualization.

cascade (configuration B), the effect of the first fiber's core offset from the center of the second fiber. Accordingly, the coupling efficiency is seen to be fairly independent of the core offset, as long as the tapered fiber's core remains within the core area of the fiber that follows. In configuration A, the slight enhancement of efficiency near the edge of the fiber (i.e., when the tapered fiber's displacement from the center of the MM fiber is  $\sim \pm 40 \mu\text{m}$ ) is not currently understood.

## 5. Fused and Tapered $N \times 1$ Combiners under Restricted-Mode Launch Condition

To predict the coupling efficiency of  $N \times 1$  combiners, we thus measured the efficiency  $\eta_T$  for several values of the taper ratio  $R$  in the system of Fig. 6 (using a single tapered fiber between the 1-m-long fibers); the results are depicted in Fig. 9. The solid curve is the best fit to the data obtained with source 2 (■). The behavior of  $\eta_T$  versus  $R$  is seen to be nearly the same for sources 1 (▲) and 2 (■), but substantially different for source 3 (●), indicating that the extent of mode filling is of importance in this regard. The numbers at the top of the figure indicate the number of fibers that can be combined in a fused and tapered bundle for a given value of  $R$ . Thus, under the restricted-mode launch conditions, it should be possible to combine the beams of several high-power, MM lasers into one bright spot. A  $19 \times 1$  combiner of this type, for example, should yield the equivalent power of six lasers at its output facet in an approximately 100- $\mu\text{m}$ -diameter spot. We thus predict that low-divergence sources (e.g., having NA less than or equal to that of sources 1 and 2), when launched into a fused and tapered MM fiber combiner, will result in

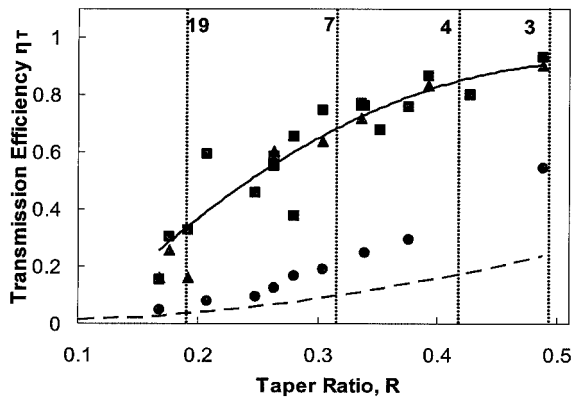


Fig. 9. Measured values of  $\eta_T$  versus the taper ratio  $R$  for a single tapered fiber in the system of Fig. 6. Light sources 1 ( $\blacktriangle$ ) and 2 ( $\blacksquare$ ) yield nearly identical patterns of behavior. The measured efficiency for source 3 ( $\bullet$ ) is substantially less than that of the other sources. Solid curve is the best fit to the data obtained with source 2. Dashed curve is the tapered fiber efficiency under fully overfilled mode launch,  $R^2$  model. Shown at the top of the figure is the number of tapered fibers that can be bundled and fused together to create an output beam equal in diameter to that of a single, standard MM fiber.

$\sim 8$  dB increase in irradiance for a  $19 \times 1$  combiner. (Note that the output étendue is  $1/19$  that of the input bundle). In contrast, the radiance theorem predicts that overfilled mode launch condition will result in no such brightness enhancement. According to the  $R^2$  model (described in Section 6) the dashed curve in Fig. 9 shows the expected efficiency of tapered fibers under fully over filled mode launch conditions. It is seen in Fig. 9 that for all values of  $R$  the efficiency of source 3 is somewhat greater than that indicated by the dashed curve, thus hinting that the modal space of source 3 is not fully occupied.

## 6. High-Order-Mode Launch Condition

Figure 9 also shows a plot of the measured transmission efficiency  $\eta_T$  of a single fiber versus the taper ratio  $R$ , when source 3 is used to provide the input beam in the system of Fig. 6 (again, with a single tapered fiber between the 1-m-long fibers). The high-spatial-mode content of the light source in this instance results in a substantial reduction of  $\eta_T$  compared with what can be achieved under restricted-mode launch conditions. For instance, at  $R = 0.193$  (corresponding to a  $19 \times 1$  fused and tapered combiner) the measured value of  $\eta_T \sim 0.06$  per laser indicates the absence of any meaningful brightness enhancement in the combined beam. This limitation, typical of overfilled mode launch condition, follows from the radiance theorem and the principle of conservation of energy.<sup>10,11</sup>

At this point it is instructive to compare our experimental results with some theoretical predictions. The transmission properties of MM optical-fiber tapers were studied by Li and Lit<sup>9</sup> in conjunction with a Lambertian source. In their geometric-optical approach, propagation in the MM fiber taper for meridional and skew rays were treated separately. They

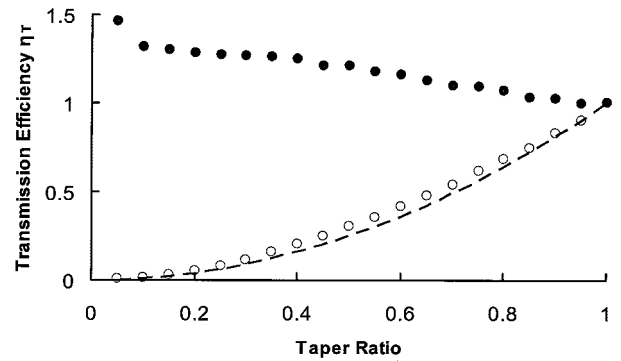


Fig. 10. Open circles ( $\circ$ ) show a single taper's transmission efficiency  $\eta_T$  versus the taper ratio  $R$  for a Lambertian source, given by Eq. (5). The dashed curve shows the taper's transmission efficiency for the overfilled mode launch condition when all modes contribute equally, namely, the  $R^2$  model. The solid circles ( $\bullet$ ) show the resulting tapered bundle's transmission improvement (i.e., the combining effect) for a Lambertian source in units of input channels calculated.

derived a formula for the skew-ray propagation and calculated the total transmitted light and the effective NA for meridional as well as skew rays. For comparison with experiments, we use their calculated effective NA and the fractional power in the skew and meridional rays. To estimate the taper efficiency, we define the average NA  $NA_R$  as the weighted sum of the effective NAs of the skew rays  $NA_{st}$  and the meridional rays  $NA_{mt}$  in the taper.

$$NA_R = f_s NA_{st} + f_m NA_{mt}, \quad (3)$$

where  $f_s$  and  $f_m$  are the corresponding weighting factors derived with the ratio  $f$  of the total light transmitted by the skew rays to the total light transmitted by the meridional rays.

$$f_s = \frac{f}{1+f}, \quad f_m = \frac{1}{1+f}. \quad (4)$$

Assuming small NAs, which is the case in our experiments, the taper efficiency  $\eta_T$  is

$$\eta_T = \left( \frac{NA_R}{NA_f} \right)^2, \quad (5)$$

where  $NA_f$  is the (uniform) fiber's NA. Figure 10 shows a plot of the taper transmission efficiency  $\eta_T$  versus the taper ratio  $R$  as predicted by Eq. (5). Also shown in the figure is a plot of the combining effect of a fiber bundle for a Lambertian source. Because the number of fibers in a tapered bundle is inversely proportional to  $R^2$ , the bundle's total (combined) efficiency in this overfilled mode case will be  $\eta_T/R^2$ . Thus, for a Lambertian source, the total combined effect is only slightly greater than unity, which is insignificant for all practical purposes.

In addition to a Lambertian source, a simple overfilled mode launch model in which modes of all orders have equal intensities can also be analyzed. For the given mode launch condition, the taper efficiency is



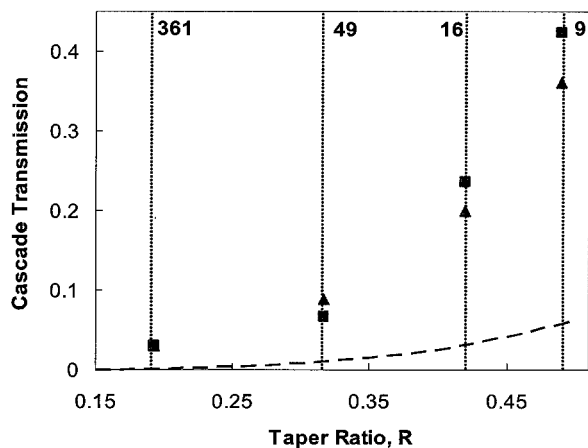


Fig. 11. Overall transmission efficiency versus taper ratio  $R$  for a cascade of two tapered fibers in the fusion-spliced chain of Fig. 6. Triangles (▲) show the data obtained with source 1. Squares (■) show the data obtained with source 2. Shown at the top of the figure, is the number  $N^2$  of fibers that can be combined together when two  $N \times 1$  combiners are connected in a cascade configuration. Dashed curve represents the cascade transmission for the overfilled mode launch condition, i.e.,  $(R^2)^2$ .

the ratio of the area of the tapered end of the fiber to the initial (untapered) area, that is,  $\eta_T = R^2$ , where  $R$  is the taper ratio. The resultant bundle's total combined efficiency for the simple overfilled mode launch is exactly equal to 1.0, and, therefore, brightness enhancement is impossible, as predicted by the well-known radiance theorem. (This result obviously does not depend on the type of fiber used for the tapers.) A plot of the taper efficiency versus  $R$  for this overfilled mode launch condition is also presented in Fig. 10 (dashed curve). The two models discussed above, the Lambertian source and the uniformly filled mode space, yield very similar efficiencies over the entire range of taper ratios.

### 7. Multistage Beam Combining by use of a Cascade of $N \times 1$ Fused and Tapered Bundles

To extend the preceding results obtained under restricted-mode launch conditions to a cascade of  $N \times 1$  combiners, we measured the transmission efficiency  $\eta_T$  versus taper ratio  $R$  for a string of two tapered MM fibers in the fusion-spliced chain of Fig. 6; the results with sources 1 (▲) and 2 (■) are shown in Fig. 11. These results indicate that essentially all the gain in brightness is obtained in the first stage of the cascade combiner, with the second stage acting primarily in the high-order-mode launch condition. Consequently, not much brightness enhancement should be expected from the second stage of the cascade configuration.

Transmission measurements on a fusion-spliced cascade of four identical  $3 \times 1$  combiners (depicted schematically in Fig. 12) showed a 22% total efficiency, namely, from each source to the output of the second stage. Although a value of  $R \sim 0.5$  is generally sufficient for  $3 \times 1$  combiners, the particular combiners used in this experiment were overpulled,

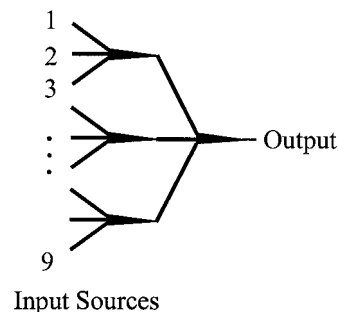


Fig. 12. Two-stage  $9 \times 1$  combiner, composed of four identical  $3 \times 1$  combiners.

resulting in a reduced taper ratio of  $R \sim 0.4$ . The measured value of  $\eta_T = 0.22$  is thus in agreement with the results depicted in Fig. 11. This means that placing nine identical lasers at the input ports of the system of Fig. 12 yields a combined output power equal to that of two lasers ( $9 \times 0.22 \sim 2$ ). Although this particular two-stage cascade of  $3 \times 1$  combiners has poor efficiency, according to the data in Fig. 11, one should be able to build a two-stage cascade of  $3 \times 1$  combiners (using  $R \sim 0.5$  tapers) with an efficiency of  $\sim 40\%$  per laser. Combination of nine identical lasers with such a device should then yield, at the output terminal, the equivalent power of 3.6 lasers.

### 8. Conclusion

We have demonstrated that beam combining with fused and tapered fiber bundles results in brightness increase under restricted-mode launch conditions (mode-filling parameter  $\sim 0.29$ ) for  $3 \times 1$ ,  $4 \times 1$ ,  $7 \times 1$ , and  $19 \times 1$  combiners. The measured values of the coupling efficiency varied approximately 1%–2% among the various fibers in each bundle, thus confirming the high quality of the fabricated devices. To analyze the performance of  $N \times 1$  combiners and cascades of such combiners, we devised a simple method employing a concatenated chain of tapered fibers in which every tapered fiber was fusion-spliced to the next fiber's unaltered facet. Good agreement between the tapered bundle efficiency estimates obtained by this method and the actual (fabricated) combiner efficiencies confirmed the validity of our approach.

For cascaded tapers with a shifted core geometry, a slight efficiency enhancement near the edge of the fiber was observed. This effect is not currently understood and requires more experimental efforts. For cascades of tapered fiber bundles, we achieved brightness enhancement only in the early stages of the cascade. We focused mainly on the dependence of the coupling efficiency on the mode-filling properties of the source. This focus enabled us to develop practical combiners in the form of fused and tapered fiber bundles and cascades of such bundles. Further experiments with controlled degrees of mode filling are left for future research. The dependence of the taper transmission efficiency on the modal content of the launched beam may be viewed from the opposite



direction, namely, the degree of mode filling in MM fibers can be estimated by measurement of the corresponding taper transmissions. This task also requires detailed taper efficiency measurements under varying mode launch conditions.

We are grateful to Shibin Jiang and Yushi Kaneda of NP Photonics, Inc. for allowing access to their experimental facilities, and to Polymicro Technologies, LLC, for providing the quartz tubes used in reported experiments. This research was supported under the Air Force Office of Scientific Research contract F49620-02-1-0380 awarded by the Joint Technology Office.

## References

1. W. A. Clarkson and D. C. Hanna, "Two mirror beam-shaping technique for high-power diode bars," *Opt. Lett.* **21**, 375–377 (1996).
2. P. Y. Wang, A. Gheen, and Z. Wang, "Beam shaping technology for laser diode arrays," in *Laser Beam Shaping III*, F. M. Dickey, S. C. Holswade and D. L. Shealy, eds., *Proc. SPIE* **4770**, 131–135 (2002).
3. D. M. Brown, "High-power laser diode beam combiner," *Opt. Eng.* **42**, 3086–3087 (2003).
4. J. Berger, D. F. Welch, W. Streifer, D. R. Scifres, N. J. Hoffman, J. J. Smith, and D. Radecki, "Fiber-bundle coupled, diode end-pumped Nd: YAG laser," *Opt. Lett.* **13**, 306–308 (1988).
5. H. Zbinden and J. E. Balmer, "Q-switched Nd: YLF laser end pumped by a diode-laser bar," *Opt. Lett.*, **15**, 1014–1016 (1990).
6. D. J. DiGiovanni and A. J. Stentz, "Tapered fiber bundles for coupling light into and out of cladding-pumped fiber devices," U.S. patent 5,864,644 (26 January 1999).
7. B. G. Fidric, V. G. Dominic, and S. Sanders, "Optical couplers for multimode fibers," U.S. patent 6, 434,302 B1 (13 August 2002).
8. J. R. Leger and W. C. Goltsoos, "Geometrical transformation of linear diode-laser arrays for longitudinal pumping of solid-state lasers," *IEEE J. Quantum. Electron.* **28**, 1088–1100 (1992).
9. Y. F. Li and W. Y. Lit, "Transmission properties of a multimode optical-fiber taper," *J. Opt. Soc. Am. A* **2**, 462–468 (1985).
10. D. H. McMahon, "Efficiency limitations imposed by thermodynamics on optical coupling in fiber-optic data links," *J. Opt. Soc. Am.* **65**, 1479–1482 (1974).
11. M. C. Hudson, "Calculation of the maximum optical coupling efficiency into multimode optical waveguides," *Appl. Opt.* **13**, 1029–1033 (1975).